Chapter 10
System Characterization and Design Using Mechanical Impedance Representations

Alexandra C. Karlicek, Brandon J. Dilworth, and J. Gregory McDaniel

Abstract Vibration testing is a critical aspect in the qualification of fieldable hardware as dynamic environments are typically design drivers, especially in the case of airborne and space-borne systems. However, when testing components or small subassemblies, it is challenging to match the boundary conditions presented by the true installation interface, which can greatly influence the outcome and inferences of a vibration test campaign. Strategically designed test fixtures, which emulate the impedance of the next level of assembly, can more effectively emulate the boundary conditions present in the fielded system. The objective of this paper is to present an approach to impedance matched fixture design, which requires matching both the transfer and output impedances of the true system. The analyses presented within this paper focus on techniques for matching the drive point impedance, which requires correct solutions for both the transfer and output impedances. The impedance matching approach will utilize undamped lumped parameter systems and highlight the advantages of characterizing the high and low frequency behavior. Additionally, closed form representations of these high and low frequency characteristics will be presented for easily realizable 1D lumped parameter systems.

Keywords Vibration testing · Impedance-matching · Mechanical impedance · Fixture design · System realizability

10.1 Introduction

Component level vibration qualification testing is typically conducted in three mutually orthogonal axes on a vibration shaker table. The input environment is normally specified as base driven input whose amplitudes are derived based on various dynamic excitation sources that are applicable to the environment in which the unit under test will operate. Common test practices dictate that the component test fixture shall provide a rigid boundary condition, and thus should not possess dynamics within the frequency bandwidth that will be tested. Although this design approach may minimize the potential for modal coupling between the test fixture and unit under test, it ultimately presents an unrealistic dynamic interface. An illustration comparing the system environment and the laboratory excitation environment is shown in Fig. 10.1. The image on the far left represents the true dynamic environment, where velocity at the base (v_1) is not equal to the velocity at the interface (v_2). On the contrary, in the test configuration $v_1 \approx v_2$ due to the aforementioned practice of designing rigid fixtures.

The issues encountered as a result of this unrealistic boundary condition include the potential for both under-testing and over-testing across the excitation bandwidth. This phenomenon has been widely recognized in the environmental testing community and is often referred to as the "impedance mismatch problem." Various strategies for mitigating these issues have been proposed which include testing techniques as well as fixture design. Test techniques include Scharton's force limited vibration testing [1] and Impedance Matched Multi-Axis Testing (IMMAT), as introduced by Daborn et al. [2]. Concepts for fixture design include Scharton's [3] multimodal design approach as well as the "N + 1" style test fixtures as investigated by Edwards [4] and Hall [5].

A. C. Karlicek (✉) · B. J. Dilworth
MIT Lincoln Laboratory, Lexington, MA, USA
e-mail: alexandra.karlicek@ll.mit.edu; brandon.dilworth@ll.mit.edu

J. G. McDaniel
Department of Mechanical Engineering, Boston University, Boston, MA, USA
e-mail: jgm@bu.edu

D. S. Epp (ed.), *Special Topics in Structural Dynamics & Experimental Techniques, Volume 5*, Conference Proceedings of the Society for Experimental Mechanics Series, https://doi.org/10.1007/978-3-030-47709-7_10

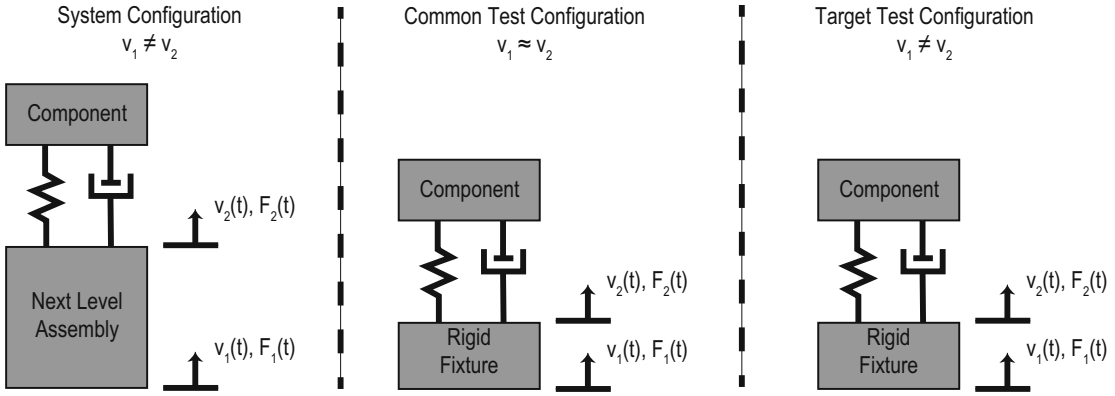

Fig. 10.1 Illustration of system and component test configurations detailing relevant interfaces

10.2 Statement

DISTRIBUTION STATEMENT A. Approved for public release. Distribution is unlimited.

This material is based upon work supported under Air Force Contract No. FA8702-15-D-0001. Any opinions, findings, conclusions or recommendations expressed in this material are those of the author(s) and do not necessarily reflect the views of the U.S. Air Force.

10.3 Background

Generically speaking, mechanical impedance refers to the ratio of the excitation force to the velocity response. An expression for the impedance of a system can be derived from the spatial model of the equation of motion for a viscously damped system, which is described by Eq. (10.1) below, where [M], [C], and [K] are NxN mass, damping, and stiffness matrices, respectively [6].

$$[M]\{\ddot{x}\} + [C]\{\dot{x}\} + [K]\{x\} = \{F(t)\} \tag{10.1}$$

Note that here N refers to the number of system equations, or number of degrees of freedom, of the system. Additionally, $\{\ddot{x}\}$, $\{\dot{x}\}$, and $\{x\}$ are Nx1 vectors of time variant acceleration, velocity, and displacement responses while $\{F\}$ is an Nx1 vector of time varying external excitation forces [6]. If $\{F(t)\} = \left\{\widetilde{F}\right\} e^{i\omega t}$, then the particular solution to (10.1) can be represented by a solution of the form $\{x(t)\} = \left\{\widetilde{x}\right\} e^{i\omega t}$, where $\widetilde{x}$ and $\widetilde{F}$ represent complex amplitudes [6].

$$\left[(i\omega)^2 [M] + i\omega [C] + [K]\right] \left\{\widetilde{x}\right\} e^{i\omega t} = \left\{\widetilde{F}\right\} e^{i\omega t} \tag{10.2}$$

This result can be rewritten in terms of the complex valued dynamic stiffness matrix, [D(ω)], which is equivalent to the ratio of force to displacement.

$$[D(\omega)] \left\{\widetilde{x}(\omega)\right\} = \left\{\widetilde{F}(\omega)\right\} \tag{10.3}$$

When the left hand side of (10.3) is rewritten in terms of velocity, the impedance matrix [Z(ω)] is found to be [D(ω)]/(iω).

$$\frac{[D(\omega)]}{i\omega} i\omega \left\{\widetilde{x}(\omega)\right\} = \left\{\widetilde{F}(\omega)\right\} \equiv [Z(\omega)] \left\{\widetilde{V}(\omega)\right\} = \left\{\widetilde{F}(\omega)\right\} \tag{10.4}$$

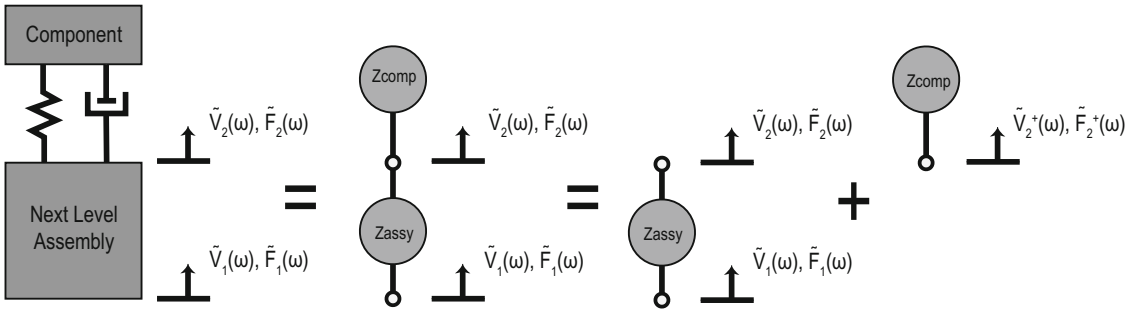

Fig. 10.2 Illustration of system configuration for impedance derivations

As the stated objective is to better emulate the true dynamic environment, then a methodology must be developed such that relative velocities v_2/v_1 presented by the system configuration, illustrated in the leftmost sketch of Fig. 10.1, match those resulting from the impedance equivalent fixture depicted in the rightmost sketch of Fig. 10.1.

First, the system is broken into lumped element representations of the assembly and component, which includes the mounting elements. This representation of the system is depicted in Fig. 10.2, where the assembly is denoted by Z_{assy} and the component is denoted by Z_{comp}. Here the assembly can be thought of as a two port mechanical system where the input, output, and transfer impedances must be considered while the component has just one impedance to be considered.

For the assembly, Z_{11} is the input impedance with $\tilde{V}_2$ set to zero and Z_{22} is the output impedance with $\tilde{V}_1$ set to zero. The reverse transfer impedance Z_{12} is $\tilde{F}_1/\tilde{V}_2$, where the input is clamped and $\tilde{F}_1$ is the force required to maintain $\tilde{V}_1$ equal to zero. Similarly, Z_{21} is the forward transfer impedance $\tilde{F}_2/\tilde{V}_1$ and $\tilde{F}_2$ is the force required to clamp the output. These relationships can be represented in matrix format as shown in (10.5).

$$\begin{Bmatrix} \tilde{F}_1 \\ \tilde{F}_2 \end{Bmatrix} = \begin{bmatrix} Z_{11} & Z_{12} \\ Z_{21} & Z_{22} \end{bmatrix} \begin{Bmatrix} \tilde{V}_1 \\ \tilde{V}_2 \end{Bmatrix} \tag{10.5}$$

The impedance of the component, as depicted in the rightmost sketch of Fig. 10.2 is simply $\tilde{F}_2^+/\tilde{V}_2^+$. When the component is connected to the next level assembly there is no external forcing applied at the interface and thus $\tilde{F}_2 = -\tilde{F}_2^+$ and $\tilde{V}_2 = \tilde{V}_2^+$. These relationships result in the system Z_{22} being replaced by $Z_{22} + Z_2$ in (10.5). Again, due to continuity at the interface between the component and assembly the ratio of $\tilde{V}_2/\tilde{V}_1$ is represented by the ratio in (10.6).

$$\frac{\tilde{V}_2}{\tilde{V}_1} = \frac{Z_{21}}{Z_{22} + Z_2} \tag{10.6}$$

Thus, in order to satisfy the condition that the dynamic behavior of the fixture match that of the higher level assembly both the output impedance Z_{22} and the transfer impedance Z_{21} must be matched. The focus of this paper will be on matching the drive point impedance, Z_d, of the system, as this solution requires all four elements of the impedance matrix in Eq. (10.5) to be properly identified.

Assuming that the force is applied at a single point, $\left\{\tilde{F}(\omega)\right\}$ has only one non-zero element. In other words $\left\{\tilde{F}(\omega)\right\} = \tilde{F}_d(\omega)\{e_n\}$, where $\{e_n\}$ is a vector whose only non-zero element represents the nth degree of freedom at which the driving force is applied. When this is substituted into (10.4) the nth element of the velocity vector $\left\{\tilde{V}(\omega)\right\}_n$ is the drive point velocity, $\tilde{V}_d$, and can be written as indicated in (10.7).

$$\left\{\tilde{V}(\omega)\right\}_n \equiv \tilde{V}_d(\omega) = \left([Z(\omega)]^{-1}\right)_{nn} \tilde{F}_d(\omega) \tag{10.7}$$

From (10.7) the drive point impedance can be expressed as shown in (10.8).

$$Z_d(\omega) \equiv \frac{1}{\left([Z(\omega)]^{-1}\right)_{nn}} = \frac{\tilde{F}_d(\omega)}{\tilde{V}_d(\omega)} \tag{10.8}$$

Assuming that [Z] is invertible, its inverse can be found by dividing the adjugate of [Z] by the determinant of [Z]. Combining this property with (10.8), an equation for the drive point impedance in terms of basic matrix operations can be written as shown in (10.9). It is clear from this representation that all four elements of (10.5) are required in order to evaluate the drive point impedance, as the determinant of the [Z] is required.

$$Z_d(\omega) = \frac{\det[Z]}{adj[Z]_{nn}} \tag{10.9}$$

As the objective of the stated impedance matching problem is to design a test fixture that provides a more realistic dynamic boundary condition, the system that satisfies the desired impedance relationship must be interpretable as a physically buildable structure.

The conversion of a desired input-output relationship into a system of interconnected mechanical elements is known as the mechanical realization problem [7]. Such an input-output relationship for a second order system is presented in Eq. (10.10), where x is an nx1 vector of displacements, u is an mx1 vector of inputs, such as external forces, and F is the nxm input influence matrix. The px1 output vector y can be written in terms of the output influence matrices of acceleration, H_a, velocity, H_v, and displacement, H_d [7].

$$\begin{aligned} [M]\{\ddot{x}\} + [C]\{\dot{x}\} + [K]\{x\} &= [F]\{u(t)\} \\ \{y\} &= [H_a]\{\ddot{x}\} + [H_v]\{\dot{x}\} + [H_d]\{x\} \end{aligned} \tag{10.10}$$

Techniques for resolving the mechanical realization problem for undamped or proportionally damped systems are well documented in the literature. These solution approaches, as detailed by Falk [8], O'Hara and Cunniff [9], and Garvey et al. [10, 11], employ transformations of the mass, stiffness, and damping matrices to satisfy the mechanically realizable constraint while preserving the desired input-output relationship.

Although the approach presented above offers a methodical process by which a mechanically realizable system with a specified behavior can be derived, it assumes initial knowledge of the target system mass, stiffness, and damping matrices. A similar body of work, known as inverse problems in vibration, utilizes specified frequency response (FRF) data to reconstruct system matrices [12]. While this generalized class of problems is more applicable to the outlined drive point impedance problem, it also relies heavily on evaluation of the system in terms of matrices, which can be computationally exhaustive.

As an alternative to matrix representations, closed form expressions for mechanical impedance can be derived using analogies to electrical circuits. Under this framework the mechanical impedance of lumped elements representing mass (m), stiffness (k), and damping (c) can be expressed as detailed in Eqs. (10.11), (10.12) and (10.13), as presented by Hixson [13].

$$Z_{mass}(\omega) = i\omega m \tag{10.11}$$

$$Z_{spring}(\omega) = \frac{k}{i\omega} \tag{10.12}$$

$$Z_{dashpot} = c \tag{10.13}$$

The equivalent drive point impedance of a network can be expressed by evaluating the connectivity of individual elements and appropriately summing their effects. The equivalent impedance of mechanical elements deemed to be in parallel (Z_p), i.e. having the same relative velocities between their connections, is simply a sum of the individual impedances. For mechanical elements in series (Z_s), i.e. having different relative velocities between their connections, the equivalent mechanical impedance is the reciprocal of the summed reciprocal impedance of individual elements [13].

$$Z_p(\omega) = \sum_{n=1}^{N} Z_n(\omega) \tag{10.14}$$

$$\frac{1}{Z_s(\omega)} = \sum_{n=1}^{N} \frac{1}{Z_n(\omega)} \tag{10.15}$$

Utilization of the rational form of the drive point impedance in order to perform system characterization is studied within the electrical community. This field of study is known as electrical network synthesis, and utilizes the rational expression of impedance or admittance, with fully defined polynomial coefficients, to determine system realizability and derive representative electrical circuit architecture [14].

10.4 Analysis

The objective of this study is to develop a methodology for designing a test fixture that matches the dynamic behavior of the next level of assembly in order to more accurately emulate the true boundary condition. As shown in the background section, this requires matching the frequency dependent output and transfer impedances. This paper will focus on the drive point impedance, as this metric encapsulates both aforementioned impedances.

The test fixture within this analysis will be represented by a lumped parameter, or discretized, model that could be used as a basis for design. To derive this lumped parameter emulator, it is assumed that the frequency dependent drive point impedance of the system of interest is available and that the low frequency, quasi-static behavior is captured. The magnitude of this impedance data then becomes the target function, where the objective is to minimize the overall Root Mean Squared Error (RMSE) between the target behavior and the analytically derived system behavior. This error minimization will be accomplished through evaluation of the topological features of the drive point impedance curve, which includes behavior at the extremes of the frequency band as well as maxima and minima.

The analysis approach to be explored within this paper focuses on undamped systems, as this solution will provide matched resonances, anti-resonances and overall frequency dependent behavior. Results from undamped systems can be extend to lightly damped systems, where a variety of damping models and can be explored to best fit the target drive point impedance signature.

For a system with N modes there are a variety of N-DOF system architectures that can provide the appropriate number of resonances. An array of architectures are considered as various configurations have the potential to provide a low error impedance match. The simplest architecture is a 1D chain, in which the initial spring-mass system is connected to ground and each subsequent spring-mass pair is connected to the $N-1$ spring mass pair. Other architectures include systems where each mass is connected to all other masses as well as ground via spring elements (all connections), systems where each mass in the chain is connected back to ground via spring elements (all grounded), and systems were some but not all masses in the chain are connected to non-adjacent masses or ground using spring elements (partial connections). An example illustration of the various architectures is provided in Fig. 10.3 for a three DOF system, where multiple partial connection systems are shown to demonstrate the variety of manners in which this architecture can be achieved.

The expression for impedance of any N degree of freedom (N-DOF) mass-spring system can be written in fractional form, using either Eq. (10.9) or Eqs. (10.11), (10.12), (10.13), (10.14) and (10.15), where the form of the polynomial expressions in the numerator and denominator can be readily predicted. The generic form of this rational expression can be most readily derived from consideration of (10.9), where each element of [Z] has the form $i\omega m + k/i\omega$, as indicated by (10.2) and (10.4). Thus, the determinant of [Z] has even powers in ω, with the highest power of ω equal to $2N$ and the adjugate of [Z] has odd powers in ω, with the highest power of ω equal to $2N-1$. Substitution of this result into (10.9) yields the general expression represented by Eq. (10.16), where the various coefficients are represented as generically as possible. Again, this result can also be realized from utilization of Eqs. (10.11), (10.12), (10.13), (10.14) and (10.15), where matrix operations are not required and thus computational advantages can be realized for large values of N.

$$\mid Z_d(\omega) \mid = \frac{\sum_{n=0}^{N} a_n \omega^{2n}}{\sum_{n=0}^{N-1} \mathrm{b}_n \omega^{2n+1}} \tag{10.16}$$

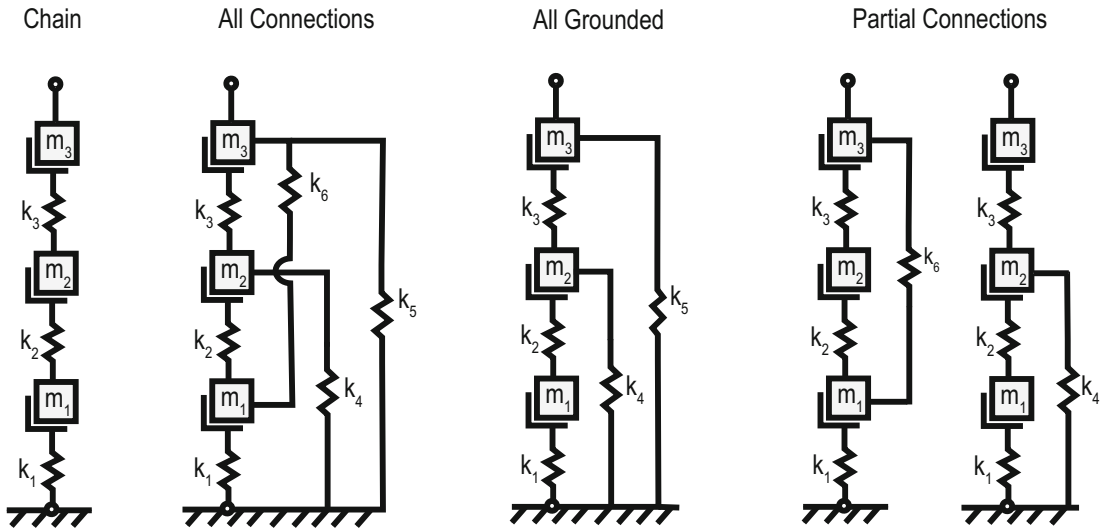

Fig. 10.3 Sample illustration of system architectures shown using 3DOF system

When expanded, Eq. (10.16) can be rewritten for MDOF systems as shown in (17), where the highest and lowest powers in both the numerator and denominator have been separated as their coefficients are of particular importance. For all of the configurations presented in Fig. 10.3, the coefficients of the highest powers in both the numerator and denominator possess only mass terms while the coefficients of the lowest powers possess only stiffness terms. The coefficients of the intermediate powers, a_n and b_n, are mixed coefficients containing combinations of both mass and stiffness elements.

$$\mid Z_d\left(\omega\right) \mid = \begin{cases} \frac{a_0\omega^{2N}+\sum_{n=1}^{N-1} a_n\omega^{2n}+a_N\omega^0}{b_0\omega^{2N-1}+b_{N-1}\omega^1} & \text{for } N \equiv 2 \\ \\ \frac{a_0\omega^{2N}+\sum_{n=1}^{N-1} a_n\omega^{2n}+a_N\omega^0}{b_0\omega^{2N-1}+\sum_{n=1}^{N-2} b_n\omega^{2n+1}+b_{N-1}\omega^1} & \text{for } N \geq 3 \end{cases} \tag{10.17}$$

As stated above, the high frequency behavior is mass dominated while the low frequency behavior is stiffness dominated, which is expressed mathematically as $a_0/b_0 = f(\{m\})$ and $a_N/b_{N-1} = f(\{k\})$. Utilizing these ratios as approximations for impedance magnitude at the extremes of the frequency domain will yield equivalency expressions in terms of target impedance modulus, frequency, and stiffness or mass, as shown in (10.18) and (10.19).

$$\alpha = \left|Z_{target}\left(\omega_{min}\right)\right| * \omega_{min} \cong \frac{a_N}{b_{N-1}} \cong f\left(\{k\}\right) \tag{10.18}$$

$$\beta = \frac{\left|Z_{target}\left(\omega_{max}\right)\right|}{\omega_{max}} \cong \frac{a_0}{b_0} \cong f\left(\{m\}\right) \tag{10.19}$$

The expressions above, which are valid for any N-DOF lumped system, can be further refined for the 1D chain architecture shown in the leftmost sketch of Fig. 10.3. This class of system is of particular interest as they are quite easily constructed and thus lend themselves to be readily leveraged for fixture design. The more specific form of (10.17) for 1D chain architectures is presented in (10.20). As indicated the a_0 and b_0 coefficients are products of the m_n discrete masses while the a_N coefficient is a product of the k_n stiffnesses. The b_{N-1} coefficient is slightly more complicated as it involves evaluation of all the possible $N-1$ combinations. For example, when the expression for b_{N-1} is evaluated for the 3DOF chain illustrated in Fig. 10.3 the result is $k_1k_2 + k_1k_3 + k_2k_3$.

$$| Z_{d_{chain}}(\omega) | = \begin{cases} \dfrac{\prod_{n=1}^{N} m_n \omega^{2N} + \sum_{n=1}^{N-1} \eta_n \omega^{2n} + \prod_{n=1}^{N} k_n}{\prod_{n=1}^{N-1} m_n \omega^{2N-1} + \omega^1 \sum_{n=1}^{N} \prod_{\substack{n=1 \\ n \neq N}}^{N} k_n} \; for \; N \equiv 2 \\ \dfrac{\prod_{n=1}^{N} m_n \omega^{2N} + \sum_{n=1}^{N-1} \eta_n \omega^{2n} + \prod_{n=1}^{N} k_n}{\prod_{n=1}^{N-1} m_n \omega^{2N-1} + \sum_{n=1}^{N-2} \mathrm{H}_n \omega^{2n+1} + \omega^1 \sum_{n=1}^{N} \prod_{\substack{n=1 \\ n \neq N}}^{N} k_n} \; for \; N \geq 3 \end{cases} \tag{10.20}$$

This result allows closed form representations of (10.18) and (10.19) to be written, where (10.21) holds exclusively for 1D chain architectures, and (10.22) is applicable to any of the topologies illustrated in Fig. 10.3.

$$\alpha = \left| Z_{target}(\omega_{min}) \right| * \omega_{min} \cong \frac{\prod_{n=1}^{N} k_n}{\sum_{n=1}^{N} \prod_{\substack{n=1 \\ n \neq N}}^{N} k_n} \tag{10.21}$$

$$\beta = \frac{\left| Z_{target}(\omega_{max}) \right|}{\omega_{max}} \cong m_N \tag{10.22}$$

In addition to assessing behavior at the extremes of the frequency band, the resonances and anti-resonances can be obtained from the target dataset. There are a variety of approaches to obtaining these frequency values, however it is recommended that established single-input-single-output (SISO) frequency domain modal fitting algorithms be utilized. Application of these algorithms to the impedance modulus will yield anti-resonant frequencies while application of these algorithms to the modulus of mobility, or 1/|Z|, will yield resonant frequencies. The number of identified resonant frequencies corresponds to the number of degrees of freedom, or lumped masses, that the emulator architecture will possess.

The resonant and anti-resonant frequencies correspond to the roots of the numerator and denominator, respectively, of Eq. (10.16). The knowledge of the roots and zeros, combined with the outputs of Eqs. (10.21) and (10.22) yields a set p equations with p unknowns, for 1D chain architectures only. For polynomials up to order four, analytic expressions for the roots can be found, and thus there are sufficient conditions by which closed form solutions can be found. This polynomial order corresponds to a 4DOF system where the substitution $\omega^2 = \lambda$ is made, such that the highest order in the numerator of (10.20) is λ^4. As analytic solutions for the roots of a polynomial with order 5 or higher do not exist, this analytic solution approach for system identification of 1D chains fails.

It is desired to evaluate 1D chains that possess more than 4DOF as well as systems of various architectures, thus a numerical solution approach is required. The most obvious approach is to conduct an exhaustive search of the various combinations of individual parameters where the impedance is calculated using Eq. (10.16) for the applicable system architecture under evaluation. The objective of this exhaustive search would be to find the combination of parameters that yields the lowest Weighted Root Mean Squared Error (WRMSE) between the target and calculated impedance modulus, where the RMSE is weighted to reflect the fact that the low amplitude values corresponding to resonances are more critical to match than the high amplitude values near anti-resonances.

Although this approach is very straightforward, it is rather limited, as large allocations of memory are required to compute the output from the various combinations of parameters. For example, a 3DOF chain architecture system with six searchable parameters would have 10^{12} possible combinations if 100 values were evaluated for each parameter. Each of these 10^{12} combinations must be computed at hundreds or thousands of frequency points, resulting in up to 10^{15} computations. Each additional degree of freedom would result in an increase in the number of computations by a power of four, assuming 100 values are investigated for each element. Another shortcoming of exhaustive search is that magnitude of the WRMSE decreases as the discretization of the parameters increases, thus driving the number of required combinations even higher if the true minimum WRMSE is desired.

In order to reduce the number of computations for an exhaustive search it is proposed that Eq. (10.18) be leveraged to determine the best combination of stiffness values to match the low frequency impedance behavior. Although this expression is presented in generality, once a specific architecture is evaluated the coefficients a_0 and b_0 can be found, or for the case of the 1D chain a closed form expression can be readily transcribed using (10.21).

As the ratio of these variables has no mass or frequency dependence (i.e. scalar), the computational expense of this calculation is quite low. The combination of stiffness values that yields the lowest WRMSE between the target and computed α values are selected and the values for the lumped masses can then be found. The value of the Nth mass can be solved for using Eq. (10.22) while the values of the remaining masses can be numerically solved for using a variety of analyses including: (1) minimizing the error between the result of Eq. (10.16) and the target impedance modulus, (2) pole and zero fitting of Eq. (10.16) or (3) solutions to the eigenvalue problem.

Although the numerical solution approaches call for exhaustive searching of the mass parameters, the utilization of stiffness dominated low frequency behavior has decoupled the stiffness parameters from this search. As a result the number of computations that are now required to minimize the error between the target and derived drive point impedances is reduced by the length of the frequency vector, $\mathcal{L}(\{\omega\})$, times the length of the mass vector, $\mathcal{L}(\{m\})$, times the length of the stiffness vector, $\mathcal{L}(\{k\})$, raised to the power of the number of springs, q. The reduction in the parameter search space by $\mathcal{L}(\{k\})^q * \mathcal{L}(\{m\}) * \mathcal{L}(\{\omega\})$ will more efficiently yield low WRMSE impedance matches for multiple system architectures, thus offering a more broad design space from which fixtures can be created.

10.5 Conclusion

A methodology for matching the drive point impedance has been proposed that leverages topological features of the impedance curve, including maxima, minima, and behavior near extremes of the frequency band. This approach offers distinct computational advantages as it decouples frequency dependence and mass parameters from the solution of the system stiffness values. Additionally, a formulation has been proposed that allows for a rational expression to be readily transcribed for both the high and low frequency behavior of easily constructed 1D chain systems. The computational advantages offered by these formulations, particularly when utilized in conjunction with the non-matrix based derivation of the drive point impedance, allows for an efficient assessment of multiple system architectures from which a broad design space for fixture design is posed.

References

1. Scharton, T.D.: Force Limited Vibration Testing Monograph. NASA RP-1403, May 1997
2. Daborn, P.M., Roberts, C., Ind, P.R. Next-generation random vibration tests. In: IMAC XXXII, the 32nd International Modal Analysis Conference, Orlando, FL, 2014
3. Scharton, T.D.: Impedance simulation vibration test fixtures for spacecraft tests. Shock Vib. Bull. **40**, (1969)
4. Edwards, T.S.: Improving boundary conditions in component-level shock and vibration tests. [Online]. Available: www.osti.gov/biblio/1146729 (2007). Accessed 23 Sept 2019
5. Hall, T.M.: Analytically investigating impedance-matching test fixtures. In: IMAC in IMAC XXXVII, the 37th International Modal Analysis Conference, Orlando, FL, 2019
6. Maia, N.M.M.: Theoretical and Experimental Modal Analysis. Research Studies Press, Baldock (1998)
7. Chen, W., Dupont, P.E.: Realization of mechanical systems from second-order models. J. Acoust. Soc. Am. **118**(2), 762–773 (2005). https://doi.org/10.1121/1.1953227
8. Falk, S.: Die Abbildung eines allgemeine schwingungssystems auf eine einfacheSchwingerkette. Ing. Arch. **23**, 312–328 (1955)
9. O'Hara, G.J, and Cunniff, P.F., "Elements of Normal Mode Theory." Naval Research Laboratory Report, 1963
10. Garvey, S.D., Friswell, M.I., Prells, U.: Coordinate transformations for second order systems. I. General transformations. J. Sound Vib. **258**(5), 885–909 (2002)
11. Garvey, S.D., Friswell, M.I., Prells, U.: Coordinate transformations for second order systems. II. Elementary structure-preserving transformations. J. Sound Vib. **258**(5), 911–930 (2002)
12. Gladwell, G.M.L.: Inverse Problems in Vibration. Kluwer Academic Publishers, Dordrecht (2004)
13. Hixson, E.L.: Mechanical impedance. In: Harris, C.M. (ed.) Shock and Vibration Handbook, pp. 10-1–10-46. McGraw-Hill, New York (1988)
14. Baher, H.: Synthesis of Electrical Networks. Wiley, Chichester (1984)